Proc. Natl. Acad. Sci. USA
Vol. 89, pp. 9504–9508, October 1992
Developmental Biology

# Retroviral analysis of cardiac morphogenesis: Discontinuous formation of coronary vessels

(heart development/cell lineage/gene transfer/smooth muscle/endothelium)

TAKASHI MIKAWA AND DONALD A. FISCHMAN

Department of Cell Biology and Anatomy, Cornell University Medical College, 1300 York Avenue, New York, NY 10021

*Communicated by Elizabeth D. Hay, July 14, 1992*

**ABSTRACT** **Cellular progenitors of the coronary vasculature are believed to enter the chicken heart during epicardial morphogenesis between stages 17 and 27 (days 3–5) of egg incubation. To trace cells which give rise to the coronary arteries *in vivo*, we applied retroviral cell tagging procedures and analyzed clonal populations of vascular smooth muscle, endothelium, and connective tissue in the hearts of post-hatch chickens. Our data provide direct proof that (*i*) vascular smooth muscle progenitors begin to enter the heart at stage 17, substantially after the heart begins propulsive contractions; (*ii*) cardiac myocytes, vascular smooth muscle, perivascular fibroblasts, and coronary endothelial cells all derive from independent precursors when these cells migrate into the heart; (*iii*) endothelial cells of the coronary vessels have a different clonal origin than endothelial cells of the endocardium; (*iv*) coronary arteries form by the coalescence of discontinuous colonies (i.e., *in situ* vasculogenesis), each derived from a founder cell tagged at the time of retroviral injection (stages 17–18); and (*v*) coronary arteries contain discrete segments composed of "polyclones." These studies indicate the feasibility of gene targeting to coronary progenitors through the use of recombinant retroviruses.**

The embryonic chicken heart begins rhythmic contractions at Hamburger–Hamilton stage 10 (≈28 hr of incubation) (1, 2), but for the first 6 days of chicken embryogenesis the myocardial wall is avascular and nourished by diffusion through the endocardium (3–5). Such diffusion is facilitated by extensive trabecular channels which markedly increase endocardial surface area (6). Overt coronary vasculogenesis begins on day 6 of incubation (stage 29), first as venous sinusoids in communication with the trabecular channels, and secondarily as coronary arterial vessels which anastomose with the sinusoids (7, 8). A closed coronary vasculature is completed after day 14 of embryogenesis (3–5). Up to stage 15, the heart is composed of only two cell types: myocytes and endothelial cells; neither connective tissue, coronary vessels, neural elements, nor the conduction system is evident histologically (9, 10). Progenitor cells of the coronary vessels along with connective-tissue precursors are believed to enter the heart as the epicardial mantle envelopes the myocardium at stages 17–27 (10–12). Except for one study using chicken–quail chimeras to trace endothelial cells in the developing avian vasculature (13), no lineage analyses of coronary progenitors have been published. In this report we present an application of retroviral cell tagging (14, 15) procedures for tracking smooth muscle, endothelial, and connective-tissue progenitors during coronary morphogenesis. We demonstrate the independence of fibroblast, smooth muscle, and endothelial lineages and prove that coronary vessels form by *in situ* vasculogenesis rather than by angiogenic outgrowth from the root of the aorta.

## MATERIALS AND METHODS

**Retroviral Vector and *in Ovo* Infection.** The retrovirus used for cell labeling, CXL, is a spleen necrosis virus-based, replication-defective virus expressing β-galactosidase. Preparation of the vector, viral propagation *in vitro*, proof of helper virus-free stocks, and the evidence for clonality in studies on myocardial development have been presented elsewhere (16, 17). When viral concentrations of $>10^7$ active virions per ml were required, culture supernatants of D17.2G/CXL187 packaging cells, containing titers of $1–3 \times 10^6$ active virions per ml, were concentrated by ultracentrifugation (17). In the present study, virus suspensions of ≈5 nl, containing Polybrene at 100 μg/ml, were pressure injected *in ovo*, into either the precardiac mesoderm at Hamburger–Hamilton (18) stages 4–9 or into the myocardial wall of beating hearts at stages 10–18. After the eggs were resealed with Parafilm, each injected embryo was returned to a humidified incubator at 37.5°C and allowed to hatch.

**Histochemistry.** One day after hatching the chicks were killed by cervical transection, and the hearts were fixed by immersion overnight at 4°C in phosphate-buffered saline containing 2% paraformaldehyde and processed for 5-bromo-4-chloro-3-indolyl β-D-galactopyranoside (X-Gal) histochemistry in whole mount as described (17). Hearts exhibiting β-galactosidase-positive colonies within the coronary vessels were embedded in paraffin, serially sectioned at 10-μm thickness, and examined by brightfield or Hoffman modulation optics. For immunoperoxidase staining, paraffin was removed with xylene, and the sections were rehydrated in decreasing ethanol concentrations and then immersed in phosphate-buffered saline containing bovine serum albumin at 1 mg/ml. Slides were stained with a mouse monoclonal antibody reactive with smooth muscle α-actin (clone 1A4, BioGenex Laboratories, San Ramon, CA) and then a goat polyclonal IgG tagged with horseradish peroxidase (HyClone). Peroxidase activity was detected by immersion for 5 min at room temperature in a solution containing diaminobenzidene at 0.2 mg/ml and 0.15% $H_2O_2$.

## RESULTS AND DISCUSSION

More than 2000 embryos were injected in this study and processed for X-Gal histochemistry. Blue-stained cells were restricted to the heart; only rarely were β-galactosidase-positive colonies detected in other tissues of the embryo, and these occurred only when >5 nl of high-titer viral supernatant was injected. When injections were performed at stage 15 or earlier (days 1 and 2 of incubation), all blue-stained cell clusters were myocytes restricted to the myocardium (17).

The publication costs of this article were defrayed in part by page charge payment. This article must therefore be hereby marked "*advertisement*" in accordance with 18 U.S.C. §1734 solely to indicate this fact.

Abbreviation: X-Gal, 5-bromo-4-chloro-3-indolyl β-D-galactopyranoside.

Labeling of coronary vascular components—smooth muscle and endothelium—as well as connective-tissue cells occurred only when embryos were injected with CXL at stage 17 (day 3) or later, and this occurred most frequently when the micropipette was placed near the dorsal mesocardium (Fig. 1*A*). We conclude that progenitors of these latter three cell populations enter the heart only at or after stage 17 and may do so near the dorsal mesocardium, as previously suggested (11, 12, 19).

When high viral titers were injected, three populations of X-Gal-stained cells were seen (Fig. 1*A*), sometimes in close proximity. However, these are unlikely to have originated from a single precursor, since when low viral titers were injected, the widely separated colonies contained cells of only a single type—i.e., the clones contained homogeneous populations (Fig. 1 *B* and *C*). In the coronary vessels these were of two types: (*i*) spirally arranged, spindle-shaped cells oriented transverse to the long axis of the vessels (type 1 cells of Fig. 1) and (*ii*) elongated, flattened cells running in the long axis of the vessels (type 2 cells of Fig. 1*A*). The type 1 cells were restricted to the tunica media (Fig. 2*A*), stained positively for smooth muscle $\alpha$-actin (Fig. 2*C*), and had a long spindle shape reminiscent of a roundworm (Fig. 2*B*). We conclude that the type 1 cells are smooth muscle. In no case was a vessel labeled over its entire length. X-Gal staining was restricted to discrete segments of a vessel and no segments >1000 $\mu$m were observed. Smooth muscle segments were typically 250–300 $\mu$m long and had remarkably sharp borders (Fig. 1 *B* and *C*). Blue-stained cells alternated with unstained cells. Assuming that every cell containing integrated retroviral DNA expressed detectable $\beta$-galactosidase, we conclude that each spiral segment must have formed from at least two or more progenitors—i.e., the blue-stained segments were polyclones. The full arguments for clonality and constitutive $\beta$-galactosidase expression are presented in a previous publication (17).

The type 2 cells were limited to the luminal surface of the tunica intima and never reacted with antibodies against smooth muscle $\alpha$-actin. We conclude that these cells were endothelia. As was the case for the smooth muscle colonies, the $\beta$-galactosidase-positive endothelial cells were restricted to defined segments of the coronary vessels but these colonies extended over much greater lengths (often >500 $\mu$m) than the smooth muscle colonies and frequently spanned branch points of the vessels (Figs. 1*A* and 3). Branching of smooth muscle colonies was observed less frequently and only in small arteries or arterioles near the apex of the heart. Labeling of coronary endothelium was clearly separable from labeling of endocardial endothelium. In none of the CXL-infected embryos did we observe single colonies with colabeled endothelium in coronary vessels and endothelium in the ventricular or atrial endocardia.

In addition to retroviral labeling of endothelial and smooth muscle precursors, $\beta$-galactosidase-positive colonies were observed in the interstitial connective tissue (Fig. 2*D*). Precise identification of these cell types was not attempted; however, in no case did we observe a single colony containing cells of mixed type. For example, no colonies were seen with both labeled endothelium and labeled smooth muscle, or with labeled smooth muscle and interstitial connective tissue. If a common progenitor gives rise to two or more of these cell types, then its lineages must have branched off prior to stage 17, when these cells enter the heart.

A model to explain our observations on coronary vasculogenesis is presented in Fig. 4. At stages 17–18 stem cells migrate into the heart wall, *en passage* with cells of the epicardium (11, 20, 21). (It should be reemphasized that no coronary vessels are present in the heart at this stage of development.) One of these stem cells is labeled by a retrovirus, and this tagged cell, upon proliferation and differentiation, gives rise to a colony of either endothelial or smooth muscle cells. In some unknown manner, polyclonal clusters

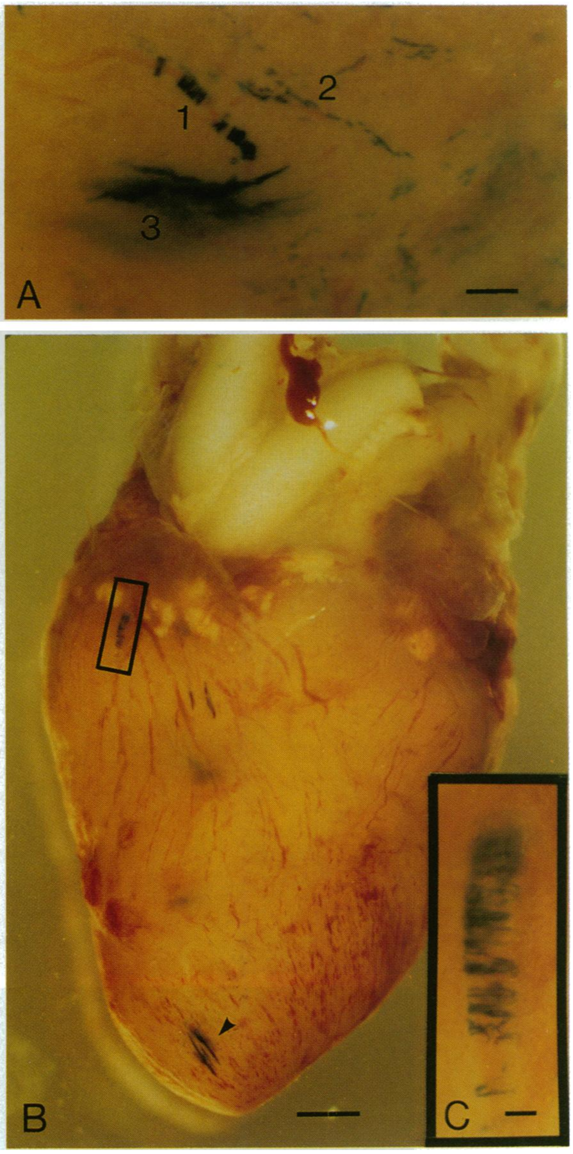


FIG. 1. Chicken embryos at stage 17 were injected *in ovo* with 5 nl of CXL viral suspensions removed from the culture supernatants of D17.2G/CXL187 cells, after addition of Polybrene (Sigma) to a final concentration of 100 $\mu$g/ml (6, 17). In some experiments (*A*) viral stocks were concentrated by centrifugation of the supernatants at 30,000 × *g* for 2–4 hr at 25°C. This achieved a viral titer of ≈3 × $10^7$ active virions per ml. Where isolated colonies were desired (*B*), unconcentrated viral suspensions (≈$10^6$ infective virions per ml) were used for embryo injection. After the opening in each shell was resealed with Parafilm, the eggs were incubated at 37.5°C. One day after hatching the hearts were removed and kept in fixative overnight at 4°C. After extensive washing in phosphate-buffered saline the whole hearts were stained *en bloc* with X-Gal and viewed under a dissecting microscope. Heart containing at least three types of morphologically distinguishable, blue-stained patches (labeled 1, 2, and 3) is seen in *A*. Colony types 1 and 2 were confined to blood vessels; type 3 was restricted to muscle of the myocardium. Each colony consisted of only a single class of cells. Type 1 colonies contained cells transversely encircling arteries and arterioles; a similar colony in a second heart has been boxed off in *B* and *C*. Type 2 colonies consisted of smaller cells running near the central axis of arteries, veins, and capillaries. Type 3 colonies were composed exclusively of cardiac myocytes. Another type 3 colony is seen near the ventricular apex in *B* (arrowhead). Note that the blue-stained cells in all three colony types were intermingled with unstained cells. (Bar = 100 $\mu$m in *A*, 800 $\mu$m in *B*, and 40 $\mu$m in *C*.)

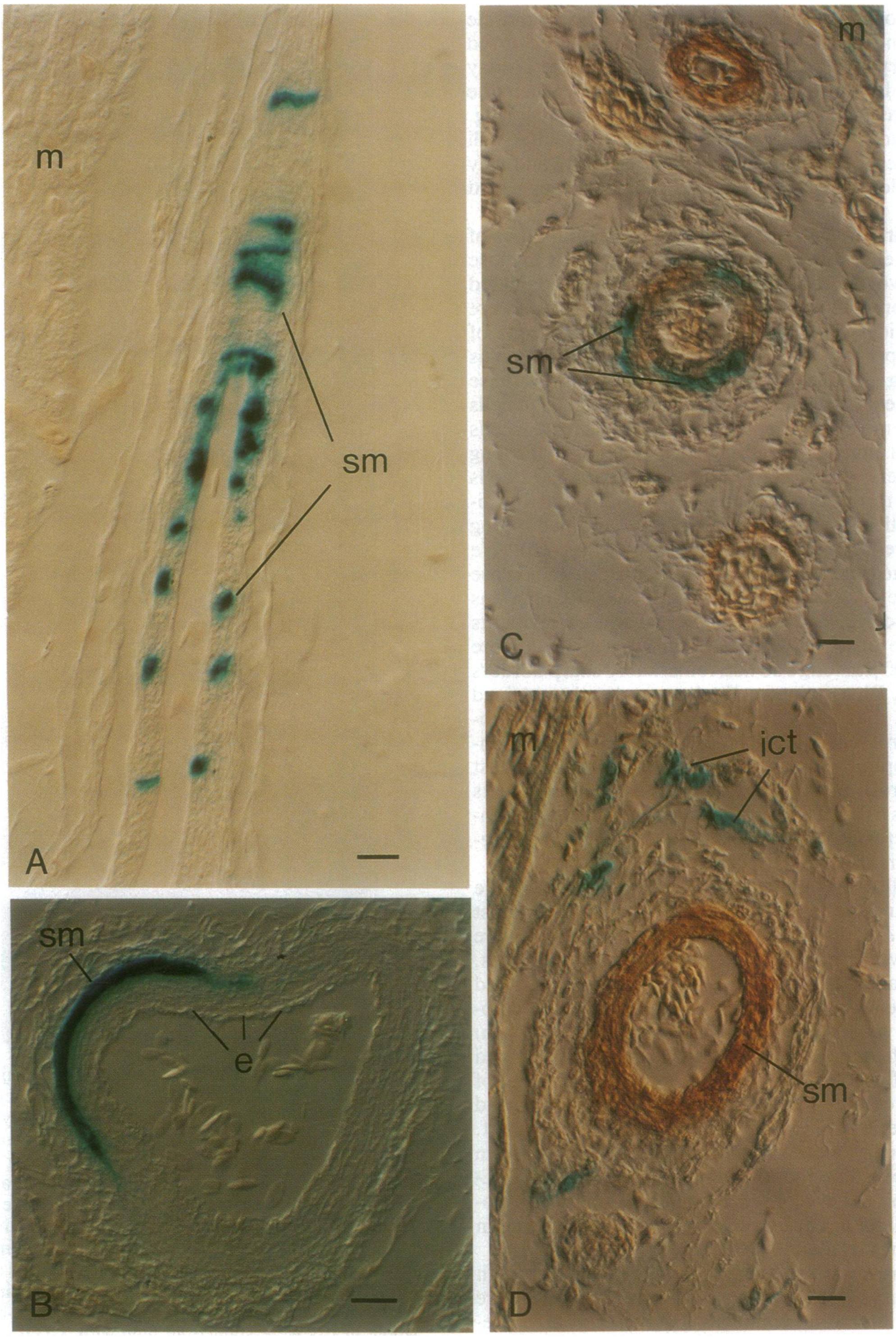


FIG. 2. Paraffin sections (10 $\mu$m thick) of selected colonies viewed under Hoffman modulation contrast. (*A*) Slightly oblique, longitudinal section of a type 1 colony. The blue-stained cells are confined to the tunica media of a small artery. Note the absence of X-Gal reaction product in the tunica adventitia and tunica intima of this vessel. (*B*) Transverse section of a type 1 colony showing virtually the complete length of a $\beta$-galactosidase-positive smooth muscle cell. Cells of the endothelium are unlabeled. (*C* and *D*) Immunoperoxidase labeling for smooth muscle $\alpha$-actin. The blue-stained cells in *C* are limited to the peroxidase-positive tunica media. Labeled cells in *D* are restricted to the interstitial connective tissue; no tagged cells are seen in the tunica intima or adventitia. Symbols: e, endothelium; sm, smooth muscle; m, cardiac myocytes; ict, interstitial connective tissue. (Bar = 20 $\mu$m.)

of smooth muscle and endothelium coalesce to form the growing vessels. The most plausible hypothesis is that the endothelial cells form sinusoidal sacs or channels with a single cell layer. Differentiating smooth muscle progenitors are attracted to these endothelial channels, possibly by a chemotactic mechanism, and then form spiral-like colonies encircling the endothelium. Omitted from the diagram is the entry of other connective-tissue elements—e.g., fibroblasts, which form the tunica adventitia. The results do not support a continuous angiogenic outgrowth model from the root of the aorta; rather, the data support a discontinuous or *in situ* (13, 22–24) model for coronary vasculogenesis. Histological analysis of early embryos is in complete agreement with this conclusion (7, 25). Not addressed by this study, but an

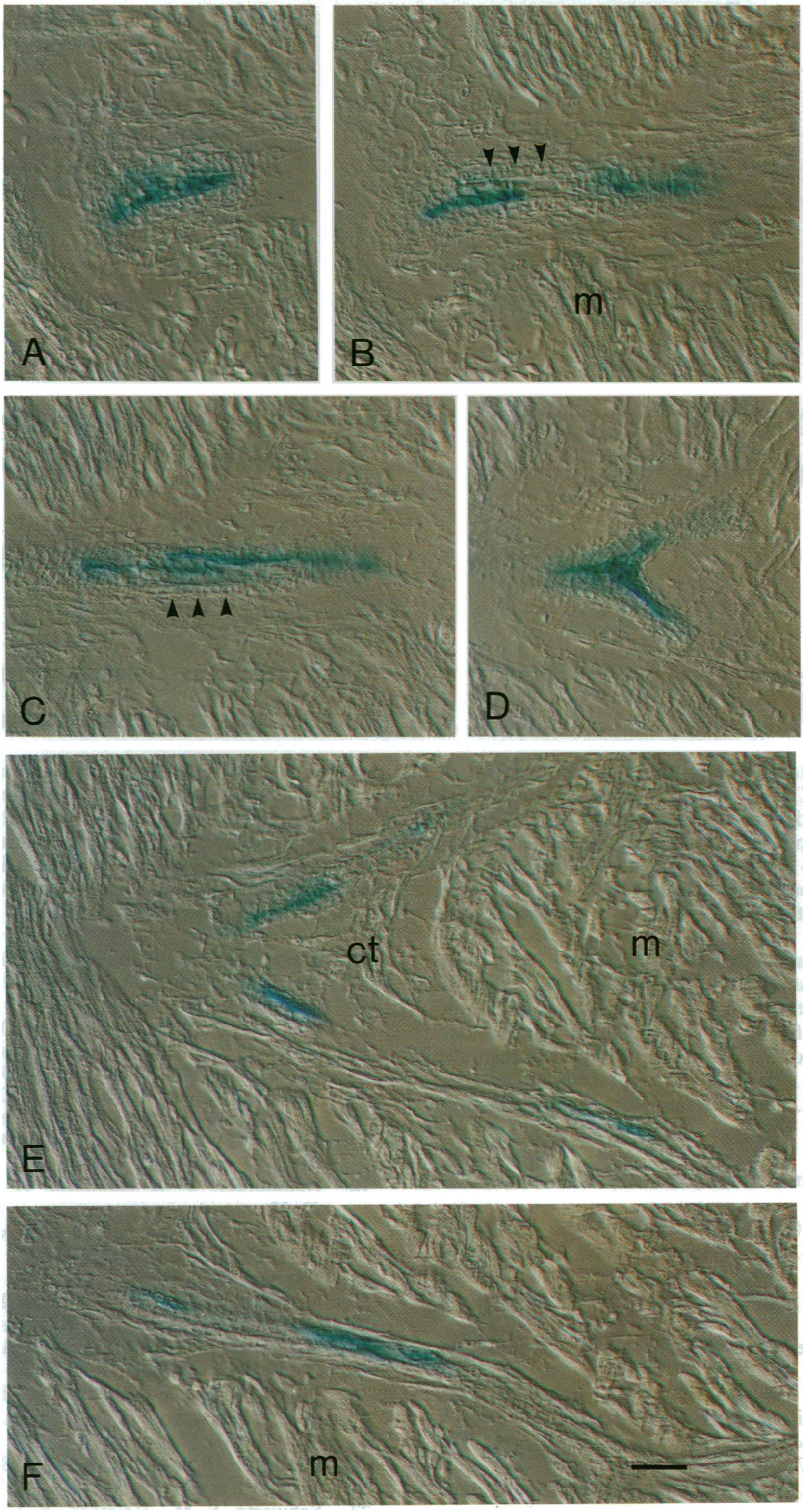


FIG. 3. Serial sections (*A–F*) of an artery containing a type 2 colony. Note the absence of X-Gal reaction product in the transversely oriented smooth muscle cells (arrowheads), in the surrounding connective tissue (ct), and in the adjacent cardiac myocytes (m). (Bar = 20 $\mu$m.)

obvious outgrowth from it, is the question: why do coronary vessels form only in certain areas of the subepicardial compartment—e.g., along the anterior interventricular sulcus? Are there restricted mitogenic and migratory signals in those regions?

Our model provides an embryological context for the monoclonality of atherosclerotic plaques first observed by Benditt and Gown (26) and reviewed by Schwartz *et al.* (27). Of a more general nature, our work demonstrates that retroviral gene targeting to cardiac myocytes and cells of the coronary vasculature is feasible in the chicken embryo. Since the grape-like clusters of cells along the dorsal mesocardium (11, 12, 20) which give rise to the epicardium can be dissected from an embryo and grafted to another host (T.M., unpublished observations), gene transfer into the vascular precursors might be facilitated by tissue immersion in larger volumes of retroviral suspension than can be realized with intraembryonic injections.

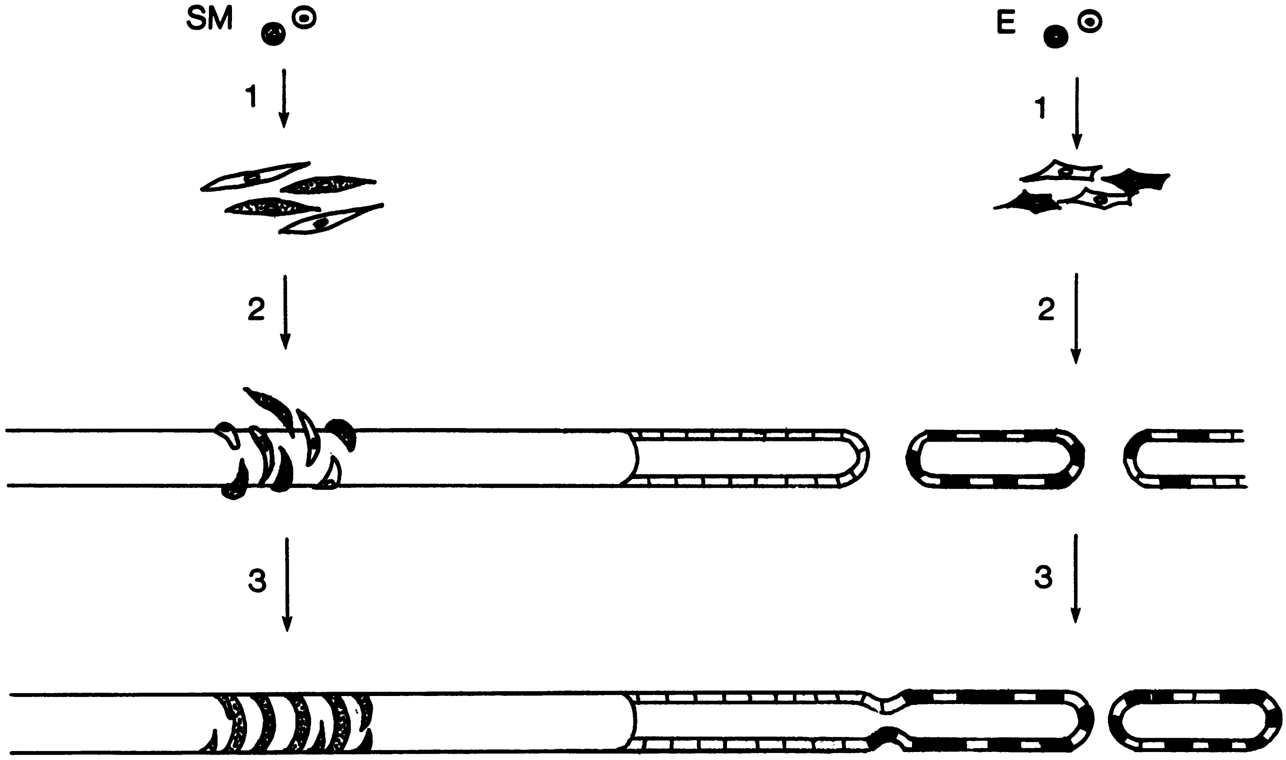


FIG. 4. Hypothetical model representing the construction of a coronary arteriole from endothelial and smooth muscle progenitors. Independent endothelial (E) and smooth muscle (SM) precursors proliferate and form identifiable clones (step 1). The endothelial cells differentiate to form sinusoidal sacs or channels (step 2). These sinusoids fuse along certain preferred axes, eventually forming capillary channels (step 3). Members of a smooth muscle clone migrate to defined segments of a channel formed by the endothelial cells (step 2) and differentiate to form the spiral segments observed with the retrovirus tagging. The tunica media and tunica intima, populated by the smooth muscle and endothelial precursors, respectively, are polyclonal—i.e., these regions are derived from more than one progenitor of each cell type. Omitted from this diagram are the other progenitors which contribute to the tunica adventitia and surrounding interstitial connective tissue.

We express our appreciation to Lydia Miroff and Lee Cohen-Gould for their technical support and to Kathleen Gallagher for secretarial assistance. We thank Drs. Drew Noden, Roger Markwald, and David Bolender for many helpful scientific discussions. This research was supported by grants from the National Institutes of Health (HL45458), the American Heart Association, and the Aaron Diamond Foundation. T.M. is an Investigator of the American Heart Association.

1. Patten, B. M. & Kramer, T. C. (1933) *Am. J. Anat.* **53**, 349–375.
2. van Mierop, L. H. S. (1967) *Am. J. Physiol.* **212**, 407–415.
3. Rychter, Z. & Ostadal, B. (1971) *Folia Morphol. (Prague)* **19**, 31–44.
4. Rychter, Z. & Ostadal, B. (1971) *Folia Morphol. (Prague)* **19**, 113–124.
5. Rychter, Z. & Jelinke, R. (1971) *Physiol. Bohemoslov.* **20**, 131–138.
6. Rychterova, V. (1971) *Folia Morphol. (Prague)* **19**, 262–272.
7. Bogers, A. J. J. C., Gittenberger-de Groot, A. C., Poelmann, R. E., Péault, B. M. & Huysmans, H. A. (1989) *Anat. Embryol. (Berlin)* **180**, 437–441.
8. Waldo, K. L., Willner, W. & Kirby, M. L. (1990) *Am. J. Anat.* **188**, 109–120.
9. Manasek, F. J. (1968) *J. Morphol.* **125**, 329–365.
10. Manasek, F. J. (1970) *Am. J. Cardiol.* **25**, 149–168.
11. Ho, E. & Shimada, Y. (1978) *Dev. Biol.* **66**, 579–585.
12. Hiruma, T. & Hirakow, R. (1989) *Am. J. Anat.* **184**, 129–138.
13. Coffin, J. D. & Poole, T. J. (1991) *Anat. Rec.* **231**, 383–395.
14. Sanes, J. R. (1989) *Trends Neurosci.* **12**, 21–28.
15. Cepko, C. (1988) *Neuron* **1**, 345–353.
16. Mikawa, T., Fischman, D. A., Dougherty, J. P. & Brown, A. M. C. (1991) *Exp. Cell Res.* **195**, 516–523.
17. Mikawa, T., Borisov, A., Brown, A. M. C. & Fischman, D. A. (1992) *Dev. Dynamics* **193**, 11–23.
18. Hamburger, V. & Hamilton, H. L. (1951) *J. Morphol.* **88**, 49–92.
19. Lough, J. W., Bolender, D. L. & Markwald, R. R. (1990) *Ann. N.Y. Acad. Sci.* **588**, 421–424.
20. Manasek, F. J. (1969) *J. Embryol. Exp. Morphol.* **22**, 333–348.
21. Manasek, F. J. (1971) *Dev. Biol.* **26**, 42–54.
22. Noden, D. M. (1989) *Am. Rev. Respir. Dis.* **140**, 1097–1103.
23. Noden, D. M. (1990) *Ann. N.Y. Acad. Sci.* **588**, 236–249.
24. Coffin, J. D. & Poole, T. J. (1988) *Development* **102**, 735–748.
25. Bogers, A. J. J. C., Gittenberger-de Groot, A. C., Dubbeldam, J. A. & Huysmans, H. A. (1989) *Acta Morphol. Neerl.-Scand.* **26**, 225–237.
26. Benditt, E. P. & Gown, A. M. (1980) *Int. Rev. Exp. Pathol.* **21**, 55–118.
27. Schwartz, S. M., Heimark, R. L. & Majesky, M. W. (1990) *Physiol. Rev.* **70**, 1177–1209.